Flow Regimes in Fine Cohesive Powders

Antonio Castellanos,[1,*] José Manuel Valverde,[1] Alberto T. Pérez,[1] Antonio Ramos,[1] and P. Keith Watson[2]
[1]*Departamento de Electrónica y Electromagnetismo, Universidad de Sevilla, 41012 Seville, Spain*
[2]*Xerox Corporation, Wilson Research Center, Webster, New York*
(Received 20 November 1997; revised manuscript received 2 June 1998)

Granular materials exhibit several regimes of behavior: plastic, inertial, fluidized, and entrained flow, but not all materials can pass through all of these states. Our concern is with the criteria that determine the transition from one regime to another and with the boundaries to the various flow regimes that these criteria define. Experimentally we have focused on fine, cohesive powders, where the interparticle cohesive force dominates over gravitational force and where entrained air can cause moving powder to become fluidized. [S0031-9007(98)08339-2]

PACS numbers: 45.70.Mg, 81.20.Ev, 83.70.Fn

The past decade has witnessed a strong interest in granular materials by the physics community, but there is an important class of granular materials that has been largely ignored in spite of its commercial importance; these materials can be classified as *fine cohesive powders*. In these powders, with particle diameters less than about 30×10^{-6} m, interparticle cohesive effects are dominant, and ambient gas plays an important role in the behavior of the powder. Granular materials display four different flow regimes: plastic behavior, inertial flow, fluidized flow, and entrained flow. Particle size, particle density, cohesivity, and gas flow determine which of these types of behavior occur.

(i) The plastic regime is characterized by a small spacing between neighboring particles. Velocities are small or zero and the stresses are independent of velocity for simple geometries. Plastic behavior determines the stability of heaps and slopes and there is an extensive literature on the subject because of its importance in civil engineering.

(ii) In the inertial regime the stresses are due to the transport of momentum by interparticle collisions. The spacing between particles is much smaller than the particle size but greater than in the plastic regime. In everyday life granular materials such as sand, sugar, and ground coffee exhibit the transition from plastic solid to inertial flow when the limit of plastic stability is reached. We note that the interstitial fluid plays no part in inertial flow.

(iii) Powders are capable of being fluidized by gas flow provided their cohesivity is not too great. In this regime the interparticle distance is of the same order of magnitude as the particle size. The interstitial fluid is the agent of transfer of momentum between particles, and fluid velocity determines the stresses in the material. The best known example of this situation is the fluidized bed, in which gas is forced through a bed of particles and the gas flow causes a pressure drop across the powder. When the pressure drop is sufficient to support the weight of the powder and to overcome the interparticle cohesive forces, the bed expands and becomes fluidized. The powder then takes on many of the properties of liquid, its upper surface remaining horizontal when the container is tilted.

(iv) A fourth regime is that of entrainment, or suspension of the particles by the gas. In this case the distance between particles is much greater than the size of the particles, the mean velocity of the material is close to the fluid velocity, and the interaction between particles is negligible. This is the case in a dust storm or a sand storm.

For each regime of granular behavior there is a dominant mechanism that determines the order of magnitude of the stresses in the bulk, and the transitions between the various flow regimes can then be obtained by comparing the magnitude of these stresses. For the plastic regime, in the absence of external stresses, the dominant stress is $\rho g h$ (ρ is the bulk density of the powder, g is the acceleration due to gravity, and h is the vertical length scale of the sample). In fine cohesive powders the interparticle cohesion may be much greater than the particle weight, and it is cohesion that determines the order of magnitude of stresses; that is why cohesive materials sometimes exhibit slopes steeper than 90°. Two mechanical properties of cohesive powders that can be measured are (i) the shear stress that will cause the powder to fracture in the absence of compressive stress and (ii) the tensile strength, i.e., the normal stress that will fracture the powder in the absence of shear. For most fine powders both quantities are of the same order of magnitude.

For low consolidation states [1,2], the tensile strength σ_t increases linearly with the consolidation stress σ_c, so that $\sigma_t = \alpha \sigma_c + \sigma_{t0}$ and α decreases as the material hardness increases. For uncharged, dry, fine particles the tensile strength at zero consolidation σ_{t0} scales as $\sigma_{t0} = \beta d_a d_p^{-2}$, where d_a is the size of the asperities, d_p is the particle diameter, and β depends on the material properties and bed voidage [2–4]. This expression is consistent with the observation that the cohesion increases as d_a increases and d_p decreases. This in turn explains the technique of reducing interparticle cohesivity by the addition of flow control additives [5] such as Aerosil (Degussa, Germany) or Cab-o-Sil (Cabot Corp., Waltham, MA). The additives consist of submicron aggregates of fumed silica nanoparticles, which are dispersed on

 0031-9007/99/82(6)/1156(4)$15.00

the powder particle surfaces. The addition of these nanoparticles results in a reduction in α because the additives are made of a hard material, and, therefore, they increase the hardness of the contacts; they also reduce the size of the contacts, thus reducing σ_{t0}.

A useful technique for estimating the cohesivity is to fluidize the powder. In order to fluidize a cohesive powder the gas flow has to overcome not only the weight of the powder, but also its tensile strength. The pressure drop across the powder at the point of fluidization is then given by $\Delta P = \rho g h + \sigma_t$. This pressure drop is also given by Carman's equation [6] $\Delta P/h = E\eta U(1-\epsilon)^2\epsilon^{-3}d_p^{-2}$, where η is the gas viscosity, U is the gas velocity, ϵ is the void fraction of the bed, and $E \sim 180$. Equating these relations we obtain the gas velocity needed for fluidization. For noncohesive powders ($\sigma_t \simeq 0$) the minimum velocity for fluidization is proportional to the square of the particle diameter. When particles are very fine the interparticle cohesive forces become dominant and the minimum velocity for fluidization becomes less dependent on the particle diameter. Referring now to Fig. 1, line A in the diagram represents the minimum velocity for fluidization as a function of particle diameter (obviously the exact location of this line depends on the cohesivity of the particles). The horizontal continuation of A on the left side of the figure represents the case of very cohesive powders, and the location of this boundary depends on the hardness of the particles and on the size of the asperities. The void fraction ϵ changes with the ratio of particle weight to interparticle cohesive force. Particles above 3×10^{-5} m in diameter pack near the random close packing limit ($\epsilon \simeq 0.45$) and therefore the slope of line A does not depend on the diameter for these large particles. Below this value ϵ increases to a maximum of about 0.8 (near the random ballistic aggregation limit). This will change slightly the shape of line A for very fine particles.

The upper limit to the fluidized zone, denoted by line B, is given by Stokes drag $U = \rho_p g d_p^2/18\eta$, where ρ_p is the particle density (gas density has been neglected). This value of gas velocity, U, is the minimum required to levitate a particle, and except for very fine powders ($d_p \leq 10^{-6}$ m) this velocity is greater than the minimum velocity for fluidization. Thus line B represents the minimum velocity for particle entrainment or suspension. As may be seen, there is a critical value of particle diameter for which the suspension velocity equals minimum fluidization velocity. Therefore, if the powder consists of particles of diameter less than this critical size, fluidization by gas flow is impossible as the particles will become entrained by the flow, rather than fluidized.

Considering now the inertial regime, according to Bagnold [7] the stresses in granular flow are proportional to the square of the velocity gradient, $\tau \sim \rho_p d_p^2(U/\delta)^2$, where δ is the extent of the shear layer and U is the velocity decrement of the material across the shear layer (we assume that in the inertial case the gas is swept along by the fast-moving particles so that U represents both gas and particle velocities). According to Savage and Hutter [8] the transition between plastic and inertial regimes is given by $\rho_p d_p^2 U^2/(P\delta^2) \geq 0.1$, where P is the total normal stress; the shear layer thickness δ scales with d_p so this transition is represented by a horizontal line such as C in Fig. 1. We see from this part of the flow regime diagram that for particles above 10^{-4} m diameter, as flow velocity is increased, the transition from plastic to inertial behavior is followed at higher flows by a transition to the fluidized regime. In contrast to this, particles between 10^{-5} and 10^{-4} m do not exhibit inertial behavior but undergo a direct transition to fluidization. Below 10^{-5} m fluidization becomes increasingly sensitive to interparticle cohesion; it also becomes very sensitive to initialization conditions, i.e., to the uniformity and degree of consolidation of the powder (see below). For these reasons the flow regime diagram has to be understood in a semiquantitative way, but the general trends of the lines indicate the approximate relationships between particle size and velocity for the various regimes and transitions.

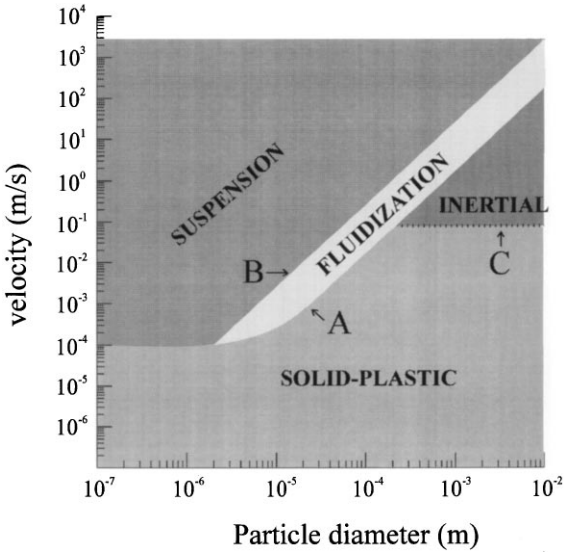

FIG. 1. Phase diagram determining the transition between flow regimes as a function of particle diameter. $\rho_p = 1000\ \mathrm{kg\,m^{-3}}$, $\eta = 2 \times 10^{-5}\ \mathrm{kg\,m^{-1}\,s^{-1}}$, $E = 180$, $g = 10\ \mathrm{m\,s^{-2}}$, $\delta = 8d_p$, $P = 1$ Pa (we assume a free moving slab, thickness ~1 mm, of toner), $h = 10$ mm, and $\epsilon = 0.5$. Values of $\alpha = 0.26$, $\beta = 0.1$, and $d_a = 1 \times 10^{-7}$ m have been taken from experimental measurements on a xerographic toner [1].

We have used the flow diagram to analyze two types of experiments: (i) the fracture and flow of powder in a tilted bed and (ii) the flow of powder in a rotating drum. In our tilted bed studies [9], we find that a typical, fine cohesive powder contains regions of widely differing degrees of consolidation, and this implies that the yield stress varies from point to point within the sample. If, however, the powder is fluidized, the dispersed material is quite uniform, and when the fluidized gas is turned

off, and as the bed collapses under its own weight, it condenses into a reproducibly consolidated state. We find that this technique, represented by line *a* in Fig. 1 provides a reliable, convenient method of initializing cohesive powders.

Having initialized the powder, we then slowly tilt the bed and observe the sample surface while maintaining the condition of zero gas flow. As the angle of tilt increases, a shear stress is generated in the powder layer, and there comes a point at which the sample fails in shear and a layer of powder slumps to one side of the bed. Experiments of this type have been carried out using a commercially available xerographic toner (Canon CLC 500 toner) and a series of Xerox toners of differing cohesivity [9]. Analyzing the breaking and sliding process by video camera and recorder indicates that if the velocity of the layer exceeds a certain critical value the moving powder becomes fluidized; this critical velocity depends on the powder cohesivity and is of the order 0.2–0.4 m/s. When the fluidized powder comes to rest it settles with its top surface horizontal, and then as the entrained air escapes the powder returns to the static, plastic state. This progression from plastic to fluidized state and back again is similar to the initialization process and is represented by line *a* in Fig. 1. This behavior contrasts with that of a coarse granular material such as sand, which breaks in a succession of inertial, surface avalanches when tilted beyond its angle of repose. This progression from plastic to inertial state, and back again, is represented by a line such as line *b* in Fig. 1.

Our rotating drum experiments also illustrate the use of the flow regime diagram and make clear the role of particle-gas interaction in the behavior of fine powders. The equipment consists of a cylindrical Plexiglas drum, designed to rotate around its axis, which is horizontal. The dimensions are 21 mm internal radius and 49 mm length. One of the ends of the cylinder has a porous filter and a connection that allows the extraction of air from the drum yet retains the particles. The drum is driven by a motor that allows a maximum angular velocity of 225 rpm. A video camera is used to record the motion, and the camera is connected to a computer for image processing. Three types of granular materials have been tested in the rotating drum: dry sand, 1.8 to 3.5×10^{-4} m diameter; xerographic toner, particle diameter around 1×10^{-5} m; and polymer beads, 3 to 5×10^{-4} m diameter, of the same resin as the toner. When the drum is partly filled with dry sand and is rotated at low velocities (~4 rpm) the sand surface is planar and makes a constant angle with the horizontal. A thin layer of material, a few grains in thickness, cascades over the surface continuously following a phase trajectory such as line *b* in Fig. 1. The slope of the surface increases with the angular velocity and at 20 rpm, the surface takes the form of tilted "S." The slope is minimum at the lower part (25°) and maximum at the upper part (64°) of the profile [see Fig. 2(a)]. This type of behavior is widely reported [10–13] for coarse, granular materials ($d_p > 10^{-4}$ m). What we observe is that the maximum angle of the slope is a continuously increasing function of the velocity, as shown in Fig. 3. The same measurements have been repeated with the chamber evacuated to 10^{-4} atm, and the results are the same as at atmospheric pressure. The same type of inertial behavior is also found when the styrene butadiene beads are tested in the rotating drum.

We have carried out the same type of experiment on fine, cohesive powders, and as one would predict from our discussion of Fig. 1, their behavior is quite different from that of sand. The powders we have studied are xerographic toners: Canon CLC 500 toner, particle diameter 8.5×10^{-6} m, and two model materials consisting of pigmented polystyrene butadiene, particle diameter 12.7×10^{-6} m, whose cohesivity has been reduced by adding 0.2% and 0.4%, respectively, by weight of the flow control additive Aerosil. Both of these toners fluidize at a superficial gas velocity of a few mm per sec.

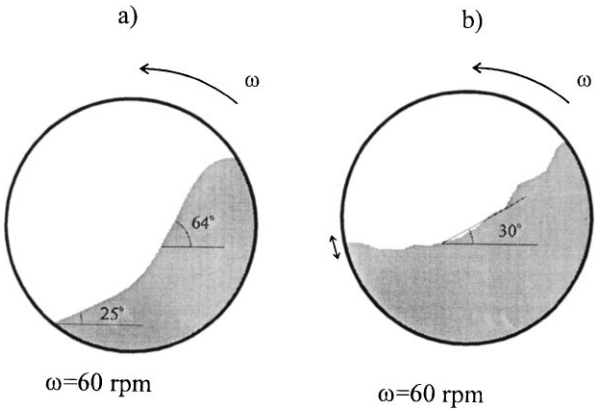

FIG. 2. (a) Profile of sand in a rotating drum. (b) Profile of toner RT (0.4% Aerosil) in the rotating drum at the same rotation velocity. Double headed arrow indicates small oscillations of the toner horizontal surface.

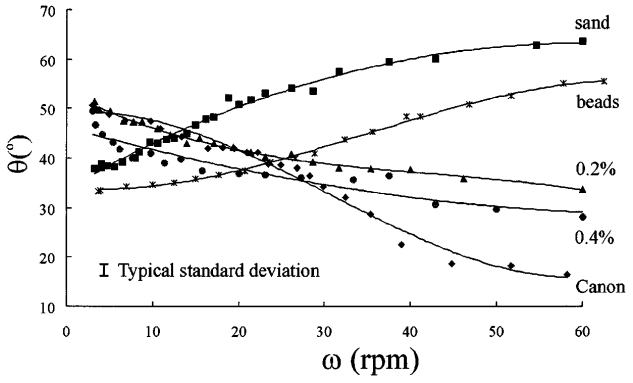

FIG. 3. Maximum angle of the slope of sand and beads (same resin as Xerox toners) and average angle of Canon CLC 500 and model Xerox toners (with 0.4% silica and 0.2% silica) at fracture as a function of rotation rate in a rotating drum at atmospheric pressure.

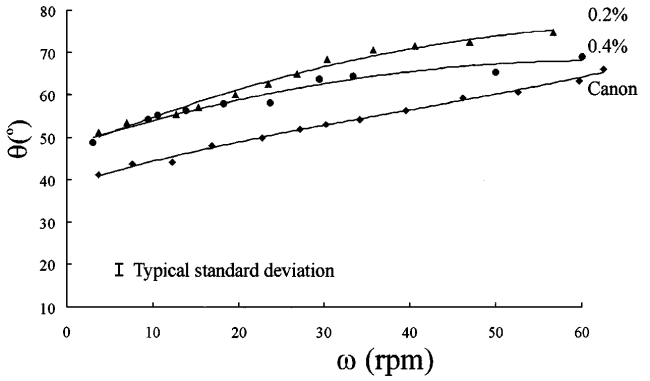

FIG. 4. Maximum angle of the slope for model Xerox toners (with 0.4% and 0.2% silica) and for Canon CLC 500 as a function of rotation rate in the rotating drum at air pressure 10^{-4} atm.

A striking feature of the toner behavior in the rotating drum is that the mean angle of the slope at fracture is a decreasing function of the angular velocity (see Fig. 3). The profiles at low speed are similar to those of sand, but as speed increases a region appears that is horizontal in the lower part of the profile [see Fig. 2(b)]. The extent of this horizontal region increases with velocity and, at the same time, the powder expands, increasing its volume considerably for velocities above 50 rpm. The reason for this behavior is that the air becomes entrained in the powder with each revolution and partially fluidizes the powder; the amount of entrained air increases with rotational velocity, and so the fluidized region increases with velocity. As we would anticipate from Fig. 1, the toner does not pass through the inertial regime but passes directly from the plastic to the fluidized condition, following line *a* in Fig. 1. This fluidized region behaves like a liquid and presents a negligible friction to the wall; therefore, the average angle of the slope decreases as the fluidized region increases with the speed of rotation.

To make clear the role of the air-particle forces in the toner flow process we have run the rotating drum while evacuating the chamber with a vacuum pump. The experiment was conducted at 10^{-4} atm. Under these conditions the toner cannot be fluidized by the residual air, and as a consequence there is a transition from the plastic regime to a system of avalanches, in a similar way to that of sand. Moreover, as shown in Fig. 4, the maximum angle of the slope is similar to that of sand. Clearly, fluidized flow requires an ambient gas, and at low gas pressure the fluidization process is suppressed. Rietema [3,14] also performed granular flow experiments in a rotating drum while varying gas pressure and observed that the angle of the slope decreases as the pressure increased. This is a clear indication that there is a progressive fluidization of the powder as the pressure increases due to the increase of the gas effective viscosity. He ascribed the decrease in slope to the entrapped gas in the powder.

In conclusion, we note that the flow regime diagram we have presented provides a useful way of interpreting the flow properties of both fine, cohesive powders and coarse granular materials. In general the motion of coarse granular material is characterized by transition from plastic to inertial flow, whereas fine particle motion at atmospheric pressure is characterized by the transition from plastic to fluidized flow. Fluidized flow, however, requires an ambient gas and at low gas pressure the fluidization process is suppressed.

We are indebted to Mike Morgan and Frank Genovese for their help and to Paul Julien for providing us the toners used in this study. This research has been supported by the Xerox Foundation, Xerox Corporation, and by the Spanish Government Agency Dirección General de Ciencia y Tecnología (DGES) under Contract No. PB96-1375.

*Corresponding author.
Email address: castella@cica.es

[1] J. M. Valverde, A. Ramos, A. Castellanos, and P. K. Watson, in *Powders & Grains 97,* edited by R. Behringer and J. T. Jenkins (Balkema, Rotterdam, 1997), pp. 163–166.
[2] J. M. Valverde, A. Ramos, A. Castellanos, and P. K. Watson, Powder Technol. **97**, 237–245 (1998).
[3] K. Rietema, *The Dynamics of Fine Powders* (Elsevier, London, New York, 1991), pp. 233–250.
[4] P. K. Watson, H. Mizes, A. Castellanos, and A. T. Pérez, in *Powders & Grains 97* (Ref. [1]), pp. 109–112.
[5] M. L. Ott and H. A. Mizes, Colloids Surf. A **87**, 245–256 (1994).
[6] P. C. Carman, Trans. Inst. Chem. Eng. **15**, 150 (1937).
[7] R. A. Bagnold, Proc. R. Soc. London A **295**, 219–232 (1966).
[8] S. B. Savage and K. Hutter, J. Fluid Mech. **199**, 177–215 (1988).
[9] J. M. Valverde, A. Ramos, A. Castellanos, and P. K. Watson, in *Powders & Grains 97* (Ref. [1]), pp. 135–138.
[10] J. Rajchenbach, Phys. Rev. Lett. **65**, 2221 (1990).
[11] G. Baumann, I. Jánosi, and D. E. Wolf, Phys. Rev. E **51**, 1879 (1995).
[12] G. H. Ristow, Europhys. Lett. **34**, 263–268 (1996).
[13] A. A. Boateng and P. V. Barr, J. Fluid Mech. **330**, 233–249 (1997).
[14] K. Rietema and W. Cottar, Powder Technol. **50**, 147–154 (1987).